

Supplemental Information

Identification of dopaminergic neurons of the substantia nigra pars compacta as a target of manganese accumulation[‡]

Gregory Robison^a, Brendan Sullivan^a, Jason R. Cannon^b, Yulia Pushkar^{*a}

^a Department of Physics and Astronomy, Purdue University, 525 Northwestern Ave., West Lafayette, IN, USA. Fax: (765)494-2970; E-mail: grobison@purdue.edu, sullivb@purdue.edu, ypushkar@purdue.edu

^b School of Health Sciences, Purdue University, 550 Stadium Dr., West Lafayette, IN, USA. Fax: (765)494-1377, Tel: (765)494-0794; E-mail: cannonjr@purdue.edu

* To whom correspondence should be addressed: Yulia Pushkar, Department of Physics and Astronomy, Purdue University, 525 Northwestern Ave, West Lafayette, IN 47907, USA. Fax: (765) 494-2970, Tel: (765) 496-3279; E-mail: ypushkar@purdue.edu

Figures

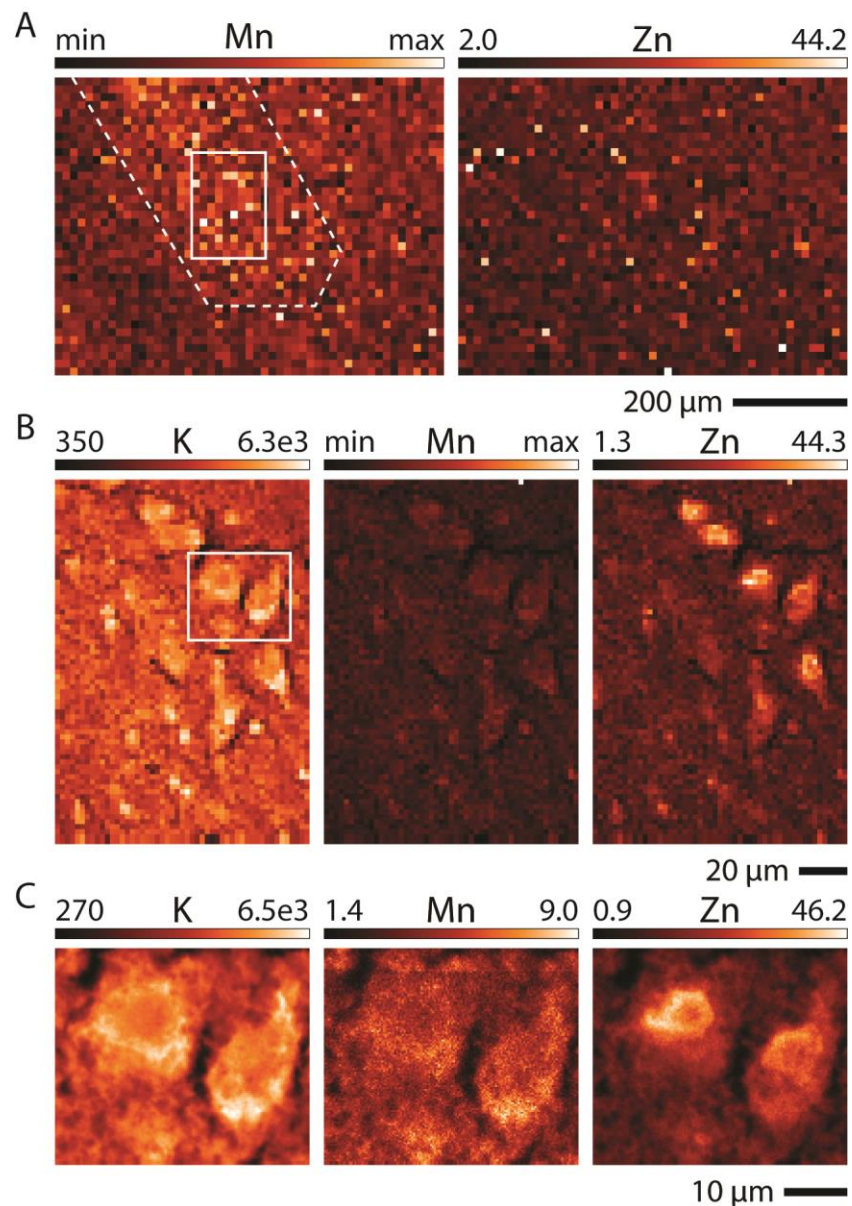


Fig. S1: Example of cell location for non-FG treated samples imaged at APS 2-ID-D. **(A)** Tissue level scan performed at $10 \mu\text{m} \times 10 \mu\text{m}$ resolution. The approximate location of the SNC is identifiable due to the increased Mn content (white dotted line). The white box indicates the approximate area scanned at $2 \mu\text{m} \times 2 \mu\text{m}$ resolution displayed in panel **(B)**. Note that at this resolution the extent of the cell body can be identified using the K signal and the Zn signal aids in identifying the extent of the nucleus. **(C)** Highest resolution scan ($0.3 \mu\text{m} \times 3 \mu\text{m}$) of two cells indicated by the white box in the preceding panel. This final images was used for subsequent analysis. Scan parameters are presented in **Table 1**. Given numbers are in $\mu\text{g g}^{-1}$.

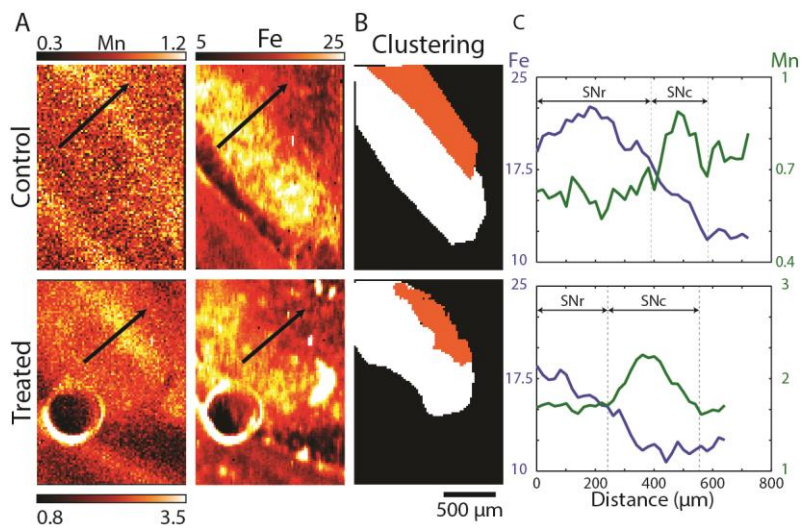


Fig. S2: Line profiles of SNC metal content. (A) XRF images of Mn and Fe displaying a line crossing the SNr/SNC boundary. (B) Based on the Mn and Fe content, the SNr (white) and SNC (orange) can be delineated by hand (control) or by k-means cluster analysis (treated). (C) The Mn line profile can be used to obtain a rough estimate of the width of the SNC (dashed gray bars). Given numbers are in $\mu\text{g g}^{-1}$.

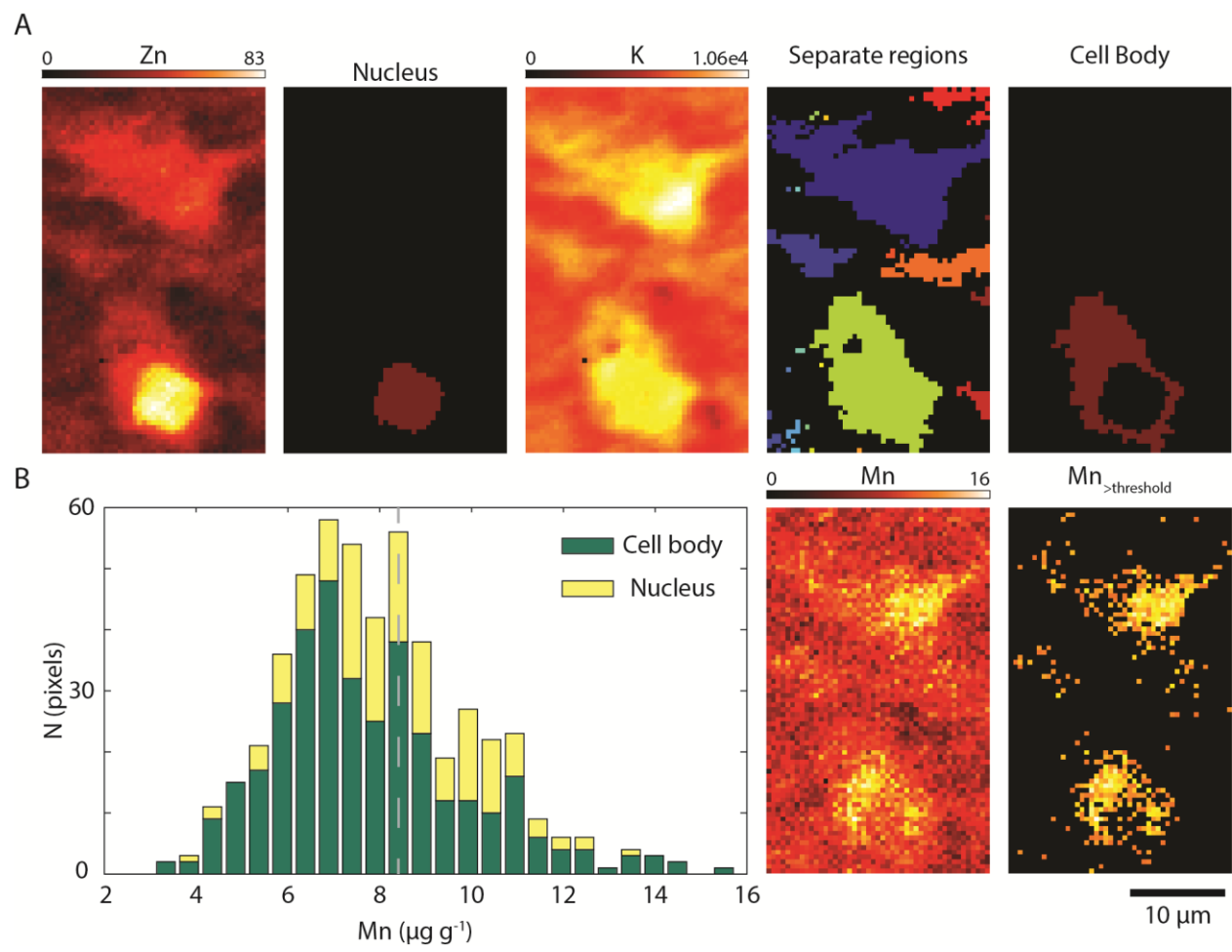


Fig. S3: Cell clustering and thresholding results. (A) Zinc image used to identify the nucleus whereas K was used in part to identify the cell body. Following clustering ($n = 3$), separate, continuous regions were identified and the region containing the nucleus selected as the cell body. (B) Stacked histogram of Mn values for the nucleus (yellow) and cell body (green). Gray dashed line indicates the threshold value and the unfiltered and filtered Mn XRF images are show for reference. Given numbers are in $\mu\text{g g}^{-1}$.

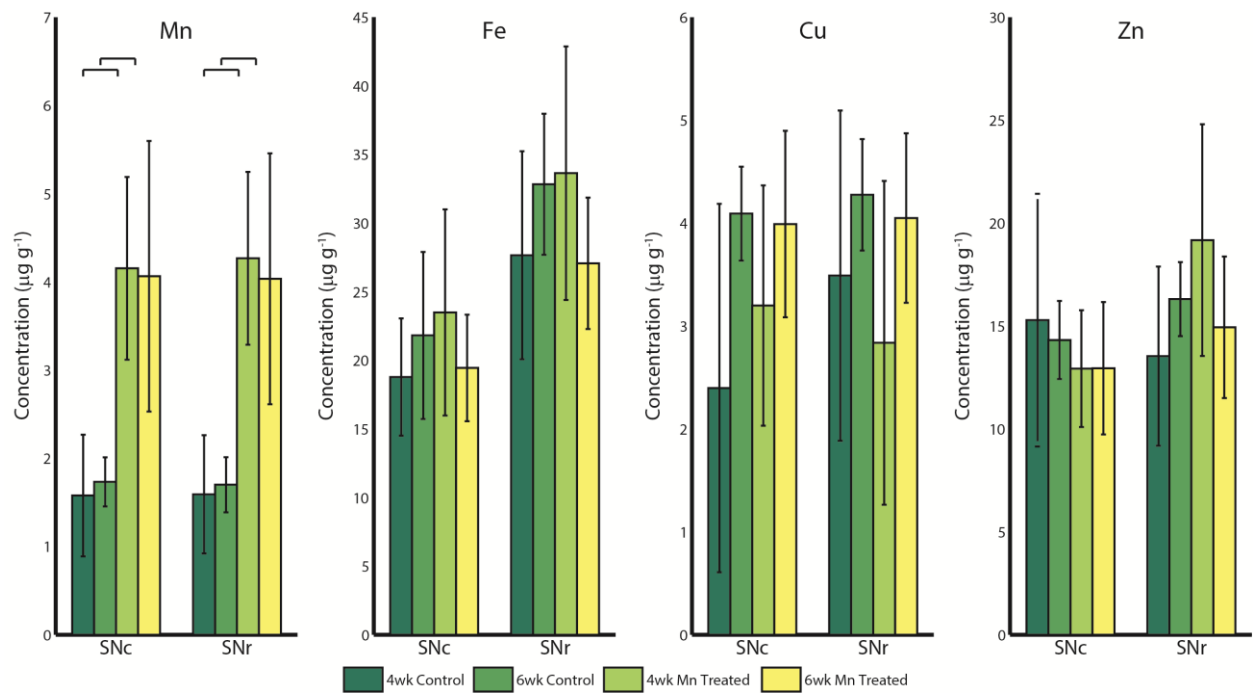


Fig. S4: SN metal content for different treatment times. Two age groups were used for this study (4 and 6 weeks); n = 6/4/8/3 animals for 4 week control/6 week control/4 week Mn treated/6 week treated respectively. Statistical significance is indicated by horizontal bars (gray, p < 0.05; black, p < 0.01). Given values represent mean \pm std in $\mu\text{g g}^{-1}$.

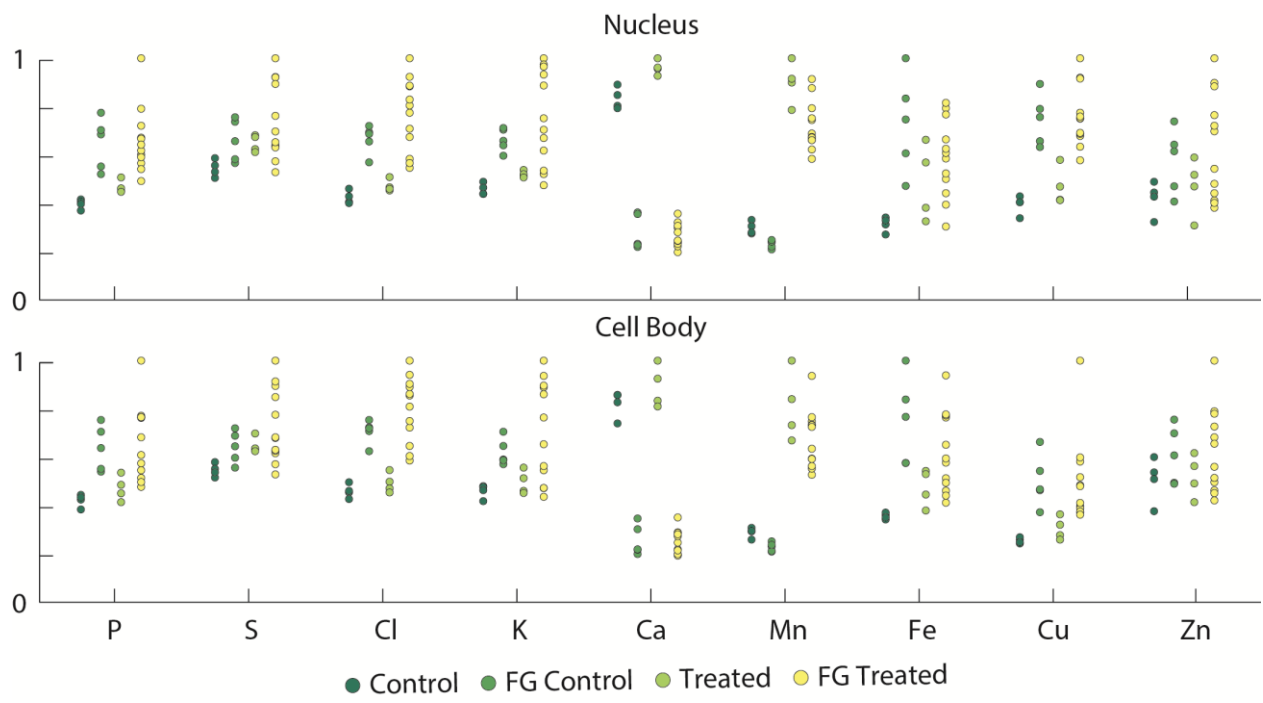


Fig. S5: Average metal concentration of SNC cells. Scatter plots showing the average metal content for all imaged SNC cells for the four experimental groups. Average metal concentration was determined for each cell and then normalized by the maximum concentration measured for the given metal. There is up to a 60% variation in metal concentration. Nucleus and cell body were separately considered.

Tables

Table S1: Metal/Mn correlations at the tissue level

Metal Group	Slope	Intercept	Pearson
	$\mu\text{g g}^{-1}$	$\mu\text{g g}^{-1}$ (mean±std)	
Fe/Mn	C ^a	13.61 ± 3.39	1.18 ± 2.46 0.26
	T	5.22 ± 1.65	1.61 ± 3.20 0.48
Cu/Mn	C ^a	2.31 ± 0.52	0.07 ± 0.39 0.94**
	T	0.69 ± 0.28	0.43 ± 0.55 0.38
Zn/Mn	C ^a	6.55 ± 1.27	2.35 ± 0.92 0.57*

^a Used upper limit concentrations for plotting
** p<0.01, * p<0.05 as compared to control.

Table S2: Cell metal concentration for nucleus and cell body

Element	All	Control	Treated	
	Non-FG	FG	Non-FG	FG
P($\times 10^3$)	2.51 ± 0.09	3.94 ± 0.54	2.90 ± 0.22	4.08 ± 0.86
K($\times 10^3$)	3.62 ± 0.21	5.04 ± 0.37	4.02 ± 0.24	5.71 ± 1.54
Mn	3.07 ± 0.25	2.40 ± 0.17	8.96 ± 1.20	7.27 ± 1.07
Fe	12.63 ± 0.50	27.87 ± 6.88	18.12 ± 4.18	23.05 ± 5.94
Cu	2.83 ± 0.16	5.54 ± 0.95	3.42 ± 0.51	5.66 ± 1.72
Zn	22.04 ± 4.68	27.81 ± 5.71	23.26 ± 4.05	28.06 ± 7.61

Given values are in $\mu\text{g g}^{-1}$ presented at mean ± std.

Table S1: Linear fit parameters for entire cell, nucleus, and cell body

Metal	Group	Non-FG Treated	Pearson	FG Treated	Pearson
		Slope	$\mu\text{g g}^{-1}/\mu\text{g g}^{-1}$	r	$\mu\text{g g}^{-1}/\mu\text{g g}^{-1}$
Entire cell					
P/Mn	C	214.4 ± 4.6 ⁺⁺	0.45**	87.0 ± 10.2 ⁺⁺	0.13**
	T	103.1 ± 2.1	0.48**	135.3 ± 2.9	0.40**
K/Mn	C	361.4 ± 5.0 ⁺⁺	0.62**	89.7 ± 9.0 ⁺⁺	0.15**
	T	161.1 ± 2.3	0.61**	166.2 ± 2.8	0.48**
Fe/Mn	C	1.29 ± 0.05 ⁺⁺	0.30**	0.86 ± 0.20	0.06**
	T	0.66 ± 0.03	0.22**	0.45 ± 0.02	0.18**
Cu/Mn	C	0.23 ± 0.01 ⁺⁺	0.23**	0.00 ± 0.09 ⁺⁺	0
	T	-0.03 ± 0.02	-0.02	-0.07 ± 0.02	-0.03
Zn/Mn	C	1.35 ± 0.05 ⁺⁺	0.28**	0.19 ± 0.07 ⁺⁺	0.04**
	T	0.90 ± 0.02	0.46**	0.67 ± 0.02	0.26**
Nucleus					
P/Mn	C	193.1 ± 7.6 ⁺⁺	0.41**	104.6 ± 17.2 ⁺⁺	0.14**
	T	110.2 ± 4.1	0.42**	96.7 ± 4.8	0.31**
K/Mn	C	271.0 ± 7.7 ⁺⁺	0.53**	84.6 ± 13.9 ⁺⁺	0.14**
	T	137.7 ± 4.0	0.51**	92.3 ± 4.2	0.34**
Fe/Mn	C	0.90 ± 0.06	0.25**	0.87 ± 0.26	0.08
	T	0.55 ± 0.07	0.13**	0.42 ± 0.04	0.16**
Cu/Mn	C	0.13 ± 0.01 ⁺⁺	0.16**	-0.27 ± 0.13 ⁺⁺	0.01
	T	0.12 ± 0.04	0.06**	-0.18 ± 0.05	0.02
Zn/Mn	C	0.54 ± 0.08 ⁺⁺	0.11**	-0.27 ± 0.13 ⁺⁺	-0.05
	T	0.012 ± 0.04	0.05**	-0.18 ± 0.05	-0.06**
Cell Body					
P/Mn	C	225.9 ± 5.8 ⁺⁺	0.48**	73.2 ± 12.3 ⁺⁺	0.12**
	T	100.5 ± 2.4	0.52**	150.9 ± 3.5	0.44**
K/Mn	C	410.3 ± 6.5 ⁺⁺	0.66**	93.7 ± 11.8 ⁺⁺	0.12**
	T	169.5 ± 2.8	0.65**	196.2 ± 3.6	0.52**
Fe/Mn	C	1.50 ± 0.06 ⁺⁺	0.32**	0.86 ± 0.30 ⁺⁺	0.06**
	T	0.70 ± 0.04	0.27	0.47 ± 0.03	0.19**
Cu/Mn	C	0.29 ± 0.01 ⁺⁺	0.26**	-0.01 ± 0.15 ⁺⁺	0
	T	-0.05 ± 0.03	-0.02	-0.12 ± 0.03	-0.05**

C, Control; T, treated

** p<0.01 as compared to a random sampling

++ p<0.01 as compared to Mn treated sample of the same non-FG/FG treatment group

References

1. O. Eschenko, S. Canals, I. Simanova and N. K. Logothetis, *Magnetic Resonance Imaging*, 2010, 28, 1165-1174.
2. S. J. Jackson, R. Hussey, M. A. Jansen, G. D. Merrifield, I. Marshall, A. MacLullich, J. L. W. Yau and T. Bast, *Behav. Brain Res.*, 2011, 216, 293-300.
3. J. Sanchez-Betancourt, V. Anaya-Martínez, A. L. Gutierrez-Valdez, J. L. Ordoñez-Librado, E. Montiel-Flores, J. Espinosa-Villanueva, L. Reynoso-Erazo and M. R. Avila-Costa, *Neurotoxicology*, 2012, 33, 1346-1355.
4. W. Zheng, Q. Q. Zhao, V. Slavkovich, M. Aschner and J. H. Graziano, *Brain Res.*, 1999, 833, 125-132.
5. R. A. Hauser, T. A. Zesiewicz, A. S. Rosemurgy, C. Martinez and C. W. Olanow, *Ann. Neurol.*, 1994, 36, 871-875.